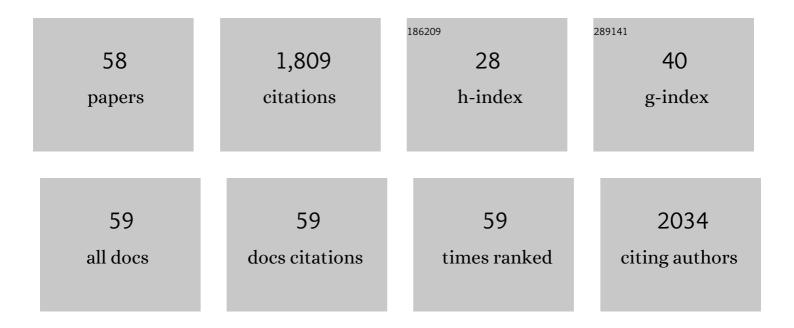
List of Publications by Year in descending order

Source: https://exaly.com/author-pdf/8506030/publications.pdf Version: 2024-02-01



<u> Βεμβους Μληίρ</u>

#	Article	IF	CITATIONS
1	Heterogeneous sono-Fenton-like process using nanostructured pyrite prepared by Ar glow discharge plasma for treatment of a textile dye. Ultrasonics Sonochemistry, 2016, 29, 213-225.	3.8	87
2	Effect of operational parameters on degradation of Malachite Green by ultrasonic irradiation. Ultrasonics Sonochemistry, 2008, 15, 1009-1014.	3.8	78
3	Heterogeneous sono-Fenton process using pyrite nanorods prepared by non-thermal plasma for degradation of an anthraquinone dye. Ultrasonics Sonochemistry, 2016, 32, 357-370.	3.8	72
4	Heterogeneous sono-Fenton-like process using martite nanocatalyst prepared by high energy planetary ball milling for treatment of a textile dye. Ultrasonics Sonochemistry, 2017, 34, 389-399.	3.8	69
5	Increasing photoactivity of titanium dioxide immobilized on glass plate with optimization of heat attachment method parameters. Journal of Hazardous Materials, 2008, 160, 508-513.	6.5	67
6	Iron rich laterite soil with mesoporous structure for heterogeneous Fenton-like degradation of an azo dye under visible light. Journal of Industrial and Engineering Chemistry, 2015, 26, 129-135.	2.9	66
7	Kinetic modeling of photoassisted-electrochemical process for degradation of an azo dye using boron-doped diamond anode and cathode with carbon nanotubes. Journal of Industrial and Engineering Chemistry, 2013, 19, 1890-1894.	2.9	61
8	Sonocatalytic degradation of Acid Blue 92 using sonochemically prepared samarium doped zinc oxide nanostructures. Ultrasonics Sonochemistry, 2016, 29, 27-38.	3.8	57
9	Photoassisted electrochemical recirculation system with boron-doped diamond anode and carbon nanotubes containing cathode for degradation of a model azo dye. Electrochimica Acta, 2013, 88, 614-620.	2.6	54
10	Photoassisted electrochemical degradation of an azo dye using Ti/RuO2 anode and carbon nanotubes containing gas-diffusion cathode. Journal of the Taiwan Institute of Chemical Engineers, 2014, 45, 930-936.	2.7	53
11	Evaluation of electrical energy per order (EEO) with kinetic modeling on the removal of Malachite Green by US/UV/H2O2 process. Desalination, 2009, 249, 99-103.	4.0	52
12	Surface imprinted CoZn-bimetalic MOFs as selective colorimetric probe: Application for detection of dimethoate. Sensors and Actuators B: Chemical, 2020, 325, 128768.	4.0	51
13	Preparation of zeolite nanorods by corona discharge plasma for degradation of phenazopyridine by heterogeneous sono-Fenton-like process. Ultrasonics Sonochemistry, 2016, 33, 37-46.	3.8	50
14	Synthesis of N-Doped Magnetic WO _{3–<i>x</i>} @Mesoporous Carbon Using a Diatom Template and Plasma Modification: Visible-Light-Driven Photocatalytic Activities. ACS Applied Materials & Interfaces, 2021, 13, 13072-13086.	4.0	43
15	Production of nanocatalyst from natural magnetite by glow discharge plasma for enhanced catalytic ozonation of an oxazine dye in aqueous solution. Journal of Molecular Catalysis A, 2015, 404-405, 218-226.	4.8	42
16	Heterogeneous sonocatalytic degradation of anazolene sodium by synthesized dysprosium doped CdSe nanostructures. Ultrasonics Sonochemistry, 2018, 40, 361-372.	3.8	42
17	Ultrasonic-assisted degradation of a triarylmethane dye using combined peroxydisulfate and MOF-2 catalyst: Synergistic effect and role of oxidative species. Journal of Molecular Liquids, 2020, 297, 111838.	2.3	41
18	Adsorption of C.I. Acid Red 97 dye from aqueous solution onto walnut shell: kinetics, thermodynamics parameters, isotherms. International Journal of Environmental Science and Technology, 2015, 12, 1401-1408.	1.8	39

#	Article	IF	CITATIONS
19	Treatment of a dye solution using photoelectroâ€fenton process on the cathode containing carbon nanotubes under recirculation mode: Investigation of operational parameters and artificial neural network modeling. Environmental Progress and Sustainable Energy, 2013, 32, 557-563.	1.3	38
20	Sonochemical synthesis of holmium doped zinc oxide nanoparticles: Characterization, sonocatalysis of reactive orange 29 and kinetic study. Journal of Industrial and Engineering Chemistry, 2016, 35, 167-176.	2.9	37
21	Combination of photocatalytic and photoelectro-Fenton/citrate processes for dye degradation using immobilized N-doped TiO2 nanoparticles and a cathode with carbon nanotubes: Central composite design optimization. Chemical Engineering and Processing: Process Intensification, 2013, 73, 103-110.	1.8	34
22	Catalytic performance of hematite nanostructures prepared by N 2 glow discharge plasma in heterogeneous Fenton-like process for acid red 17 degradation. Journal of Industrial and Engineering Chemistry, 2017, 50, 86-95.	2.9	33
23	One-step preparation of nanostructured martite catalyst and graphite electrode by glow discharge plasma for heterogeneous electro-Fenton like process. Journal of Environmental Management, 2017, 199, 31-45.	3.8	33
24	Kinetic modeling of a triarylmethane dye decolorization by photoelectro-Fenton process in a recirculating system: Nonlinear regression analysis. Chemical Engineering Research and Design, 2014, 92, 362-367.	2.7	32
25	Mg and La Co-doped ZnO Nanoparticles Prepared by Sol–gel Method: Synthesis, Characterization and Photocatalytic Activity. Periodica Polytechnica: Chemical Engineering, 2019, 64, 61-74.	0.5	32
26	Mesoporous MIP-capped luminescent MOF as specific and sensitive analytical probe: application for chlorpyrifos. Mikrochimica Acta, 2020, 187, 673.	2.5	31
27	Development of an empirical kinetic model for sonocatalytic process using neodymium doped zinc oxide nanoparticles. Ultrasonics Sonochemistry, 2016, 29, 146-155.	3.8	30
28	Preparation of a Green Photocatalyst by Immobilization of Synthesized ZnO Nanosheets on Scallop Shell for Degradation of an Azo Dye. Current Nanoscience, 2014, 10, 684-694.	0.7	29
29	Kinetic Modeling of Photocatalytic Degradation of an Azo Dye Using Nano-TiO ₂ /Polyester. Environmental Engineering Science, 2012, 29, 957-963.	0.8	28
30	Electrochemical and photo-assisted electrochemical treatment of the pesticide imidacloprid in aqueous solution by the Fenton process: effect of operational parameters. Research on Chemical Intermediates, 2016, 42, 855-868.	1.3	27
31	N-doped graphitic carbon as a nanoporous MOF-derived nanoarchitecture for the efficient sonocatalytic degradation process. Separation and Purification Technology, 2021, 256, 117811.	3.9	27
32	Kinetic modeling of sonocatalytic degradation of reactive orange 29 in the presence of lanthanide-doped ZnO nanoparticles. Ultrasonics Sonochemistry, 2017, 34, 98-106.	3.8	26
33	CdSe quantum dots-sensitized chemiluminescence system and quenching effect of gold nanoclusters for cyanide detection. Spectrochimica Acta - Part A: Molecular and Biomolecular Spectroscopy, 2019, 212, 322-329.	2.0	26
34	Synthesis, Characterization and Immobilization of ZnO Nanosheets on Scallop Shell for Photocatalytic Degradation of an Insecticide. Science of Advanced Materials, 2015, 7, 806-814.	0.1	25
35	Integration of Polydopamine and Fe ₃ O ₄ Nanoparticles with Graphene Oxide to Fabricate an Efficient Recoverable Catalyst for the Degradation of Sulfadiazine. Industrial & Engineering Chemistry Research, 2020, 59, 183-193.	1.8	24
36	Specific Fluorescence Probe for Direct Recognition of Dimethoate Using Molecularly Imprinting Polymer on ZnO Quantum Dots. Journal of Fluorescence, 2017, 27, 1339-1347.	1.3	23

#	Article	IF	CITATIONS
37	Computational study on the ability of functionalized graphene nanosheet for nitrate removal from water. Chemical Physics, 2018, 511, 20-26.	0.9	23
38	Design equation with mathematical kinetic modeling for photooxidative degradation of C.I. Acid Orange 7 in an annular continuous-flow photoreactor. Journal of Hazardous Materials, 2009, 165, 168-173.	6.5	18
39	Synthesis and characterization of gold nanoparticles usingHypericum perforatumandNettleaqueous extracts: A comparison with turkevich method. Environmental Progress and Sustainable Energy, 2019, 38, 508-517.	1.3	16
40	Self-cleaning acrylic water-based white paint modified with different types of TiO2 nanoparticles. Pigment and Resin Technology, 2016, 45, 24-29.	0.5	15
41	Fluidized-bed Fenton-like oxidation of a textile dye using natural magnetite. Research on Chemical Intermediates, 2016, 42, 8083-8095.	1.3	14
42	Inhibition of rhodamine B–ferricyanide chemiluminescence by Au nanoparticles toward the sensitive determination of mercury (II) ions. Microchemical Journal, 2016, 126, 326-331.	2.3	14
43	Development of kinetic models for photoassisted electrochemical process using Ti/RuO2 anode and carbon nanotube-based O2-diffusion cathode. Electrochimica Acta, 2016, 187, 300-311.	2.6	14
44	Sonocatalytic ozonation, with nano-TiO2 as catalyst, for degradation of 4-chloronitrobenzene in aqueous solution. Research on Chemical Intermediates, 2015, 41, 7029-7042.	1.3	13
45	Central composite design optimization of pilot plant fluidized-bed heterogeneous Fenton process for degradation of an azo dye. Environmental Technology (United Kingdom), 2016, 37, 2703-2712.	1.2	13
46	Treatment of an Azo Dye by Citrate Catalyzed Photoelectro-Fenton Process Under Visible Light using Carbon Nanotube-polytetrafluoroethylene Cathode. Current Nanoscience, 2013, 9, 387-393.	0.7	13
47	Photocatalytic degradation of an azo dye using immobilised TiO2 nanoparticles on polyester support: central composite design approach. Micro and Nano Letters, 2011, 6, 958.	0.6	12
48	Comparative study of sonocatalytic process using MOF-5 and peroxydisulfate by central composite design and artificial neural network. Journal of Molecular Liquids, 2020, 316, 113801.	2.3	12
49	An efficient chemiluminescence system based on mimic CuMOF/Co3O4 nanoparticles composite for the measurement of glucose and cholesterol. Sensors and Actuators B: Chemical, 2021, 348, 130690.	4.0	12
50	A comparative study of photocatalytic degradation and mineralisation of an azo dye using supported and suspended nano-TiO ₂ under UV and sunlight irradiations. Pigment and Resin Technology, 2016, 45, 119-125.	0.5	11
51	Scrutinizing the vital role of various ultraviolet irradiations on the comparative photocatalytic ozonation of albendazole and metronidazole: Integration and synergistic reactions mechanism. Journal of Environmental Management, 2020, 272, 111044.	3.8	10
52	Response surface optimization of heterogeneous Fenton-like degradation of sulfasalazine using Fe-impregnated clinoptilolite nanorods prepared by Ar-plasma. Research on Chemical Intermediates, 2017, 43, 3989-4005.	1.3	9
53	Optimization of a textile dye degradation in a recirculating fluidized-bed reactor using magnetite/S ₂ O ₈ ^{2â^'} process. Environmental Technology (United) Tj ET	Qq11120.78	343 〕 4 rgBT /⊂
54	Degrading a mixture of three textile dyes using photo-assisted electrochemical process with BDD anode and O2–diffusion cathode. Environmental Science and Pollution Research, 2014, 21, 8543-8554.	2.7	7

#	Article	IF	CITATIONS
55	Production of martite nanoparticles with high energy planetary ball milling for heterogeneous Fenton-like process. RSC Advances, 2016, 6, 81219-81230.	1.7	6
56	Effect of dye chemical structure on the efficiency of photoassisted electrochemical degradation using a cathode containing carbon nanotubes and a Ti/RuO2 anode. Research on Chemical Intermediates, 2015, 41, 6073-6085.	1.3	5
57	Hydrogen production from co-gasification of asphaltene and plastic. Petroleum Science and Technology, 2019, 37, 1905-1909.	0.7	3
58	Development of an Empirical Kinetics Model for Sono-Degradation of Malachite Green: Evaluation of Electrical Energy Per Order. Jundishapur Journal of Health Sciences, 2016, 8, .	0.1	1